

**OPTICALLY THIN LIQUID WATER CLOUDS:  
THEIR IMPORTANCE AND OUR CHALLENGE**

D. D. Turner, A. M. Vogelmann, R. T. Austin, J. C. Barnard, K. Cady-Pereira,  
J. C. Chiu, S. A. Clough, C. Flynn, M. M. Khaiyer, J. Liljegren, K. Johnson,  
B. Lin, C. Long, A. Marshak, S. Y. Matrosov, S. A. McFarlane, M. Miller,  
Q. Min, P. Minnis, W. O'Hirok, Z. Wang, and W. Wiscombe

January 2006

Submitted to  
Bulletin of the American Meteorological Society

**Environmental Sciences Department/Atmospheric Sciences Division**

**Brookhaven National Laboratory**

P.O. Box 5000  
Upton, NY 11973-5000  
[www.bnl.gov](http://www.bnl.gov)

# Optically Thin Liquid Water Clouds: Their Importance and Our Challenge

D.D. Turner<sup>1</sup>, A.M. Vogelmann<sup>2</sup>,  
R.T. Austin<sup>3</sup>, J.C. Barnard<sup>4</sup>, K. Cady-Pereira<sup>5</sup>, J.C. Chiu<sup>6</sup>, S.A. Clough<sup>5</sup>,  
C. Flynn<sup>4</sup>, M. M. Khaiyer<sup>7</sup>, J. Liljegren<sup>8</sup>, K. Johnson<sup>2</sup>, B. Lin<sup>9</sup>, C. Long<sup>4</sup>,  
A. Marshak<sup>10</sup>, S. Y. Matrosov<sup>11</sup>, S.A. McFarlane<sup>4</sup>, M. Miller<sup>2</sup>, Q. Min<sup>12</sup>,  
P. Minnis<sup>9</sup>, W. O'Hirok<sup>13</sup>, Z. Wang<sup>14</sup>, and W. Wiscombe<sup>2,10</sup>

<sup>1</sup> University of Wisconsin – Madison

<sup>2</sup> Brookhaven National Laboratory

<sup>3</sup> Colorado State University

<sup>4</sup> Pacific Northwest National Laboratory

<sup>5</sup> Atmospheric and Environmental Research, Inc.

<sup>6</sup> University of Maryland Baltimore County

<sup>7</sup> AS&M, Inc., Hampton, VA

<sup>8</sup> Argonne National Laboratory

<sup>9</sup> NASA Langley Research Center

<sup>10</sup> NASA Goddard Space Flight Center

<sup>11</sup> NOAA/Environmental Technology Laboratory

<sup>12</sup> State University of New York – Albany

<sup>13</sup> University of California Santa Barbara

<sup>14</sup> University of Wyoming

Submitted to the

*Bulletin of the American Meteorological Society*

**Last Modified on 18 Jan 2006**

*Corresponding author address:* Dr. David D. Turner, University of Wisconsin-Madison, 1225 West Dayton Street, Madison, WI 53706. *Tel:* (608)-263-1061, *Fax:* (608) 262-5957, *e-mail:* dturner@ssec.wisc.edu

Key words: Cloud retrievals, Intercomparison, CLOWD

## **Abstract**

Many of the clouds important to the Earth's energy balance, from the tropics to the Arctic, are optically thin and contain liquid water. Longwave and shortwave radiative fluxes are very sensitive to small perturbations of the cloud liquid water path (LWP) when the LWP is small (i.e.,  $< 100 \text{ g m}^{-2}$ ) and, thus, the radiative properties of these clouds must be well understood to capture them correctly in climate models. We review the importance of these thin clouds to the Earth's energy balance, and explain the difficulties in observing them. In particular, because these clouds are optically thin, potentially mixed-phase, and often broken (i.e., have large 3-D variability), it is challenging to retrieve their microphysical properties accurately. We describe a retrieval algorithm intercomparison that was conducted to evaluate the issues involved. The intercomparison included eighteen different algorithms to evaluate their retrieved LWP, optical depth, and effective radii. Surprisingly, evaluation of the simplest case, a single-layer overcast cloud, revealed that huge discrepancies exist among the various techniques, even among different algorithms that are in the same general classification. This suggests that, despite considerable advances that have occurred in the field, much more work must be done, and we discuss potential avenues for future research.

## **Capsule sentence**

Many clouds important to the Earth's energy balance are optically thin and contain liquid water. Despite many improvements, observations of their liquid water amount and particle size have large differences that must be resolved.

Clouds play a critical role modulating the radiative transfer in the atmosphere, and how clouds interact with the atmosphere and impact the Earth's radiative energy balance is one of the primary uncertainties in global circulation model (GCM) simulations of CO<sub>2</sub> doubling (IPCC, 2001, Stephens et al. 2002). With advances in radiative transfer modeling, it is now reasonable to assume that most errors in estimating the impact of clouds on the radiative field can be attributed to the description of cloud properties used in the models, rather than treatment of the radiative transfer physics. Low-level, liquid water clouds are arguably the simplest type of cloud to observe and have generally been thought of as being a solved problem. However, results reported here indicate that huge discrepancies exist among different observation techniques for even a simple case.

This paper is one in a series that highlight the achievements that have occurred in remotely observing cloud properties, and addresses the current issues that remain. For reasons that will be discussed, we limit the focus of this paper to clouds that contain small amounts of liquid water. While these clouds are common and are among the simplest to treat, they are misleadingly difficult to observe accurately. Our purpose is to discuss the importance of these clouds to climate, consider the challenges that must be met for their study, and describe a recent cloud property retrieval intercomparison designed to meet these challenges. The results from the intercomparison suggest that we are further than we may have expected from accurately observing these cloud properties, and that a concerted effort is needed to rectify these discrepancies.

## **The Importance of Optically Thin Water Clouds**

The description of clouds needed for climate studies requires both their microphysical properties, such as their liquid-water content and drop size distribution, and properties that are used to describe their interaction with radiation, such as their optical depth and effective radius. (See the sidebar “*Cloud Microphysics and Remote Sensing*” for a brief summary of commonly used microphysical and radiative properties and their interrelationships.) We focus our attention here on liquid-water clouds that reside at the optically thinner end of the spectrum, having a LWP less than  $100 \text{ gm}^{-2}$ . These clouds are common and are relatively simple to address compared to upper tropospheric cirrus clouds, for example. This is because liquid-water clouds tend to reside lower in the atmosphere, which makes them easier to study by surface remote sensing. They are also composed of spherical water drops whose scattering properties are described well by Mie theory (Mie, 1908), unlike ice clouds that may contain multiple crystal shapes and require much more complicated scattering treatments.

Although these clouds might not be as eye-catching as those that are central to extreme weather events, their extensive coverage means that they cannot be ignored. Analyses from the International Satellite Cloud Climatology Project (ISCCP) reveal that the global mean cloud fractional coverage is 68.6% (Rossow and Schiffer, 1999), but deep convective clouds cover only 2.6% of the globe. However, the ISCCP study found that low-level and mid-level clouds, which often contain liquid water, have mean water paths of only  $51$  and  $60 \text{ gm}^{-2}$ , respectively, and cover 27.5% and 19% of the globe. This general result from ISCCP is supported by surface observations from the Climate Research Facilities (CRFs) operated by the U.S. Department of Energy’s Atmospheric Radiation Measurement (ARM) Program, which are strategically located in different climate regimes. The distribution of LWP at a continental mid-latitude site reveals

that over 50% of the liquid-water clouds have LWPs below  $100 \text{ gm}^{-2}$  (Marchand et al., 2003). Also, approximately 80% of the liquid-bearing clouds in the Arctic have LWPs below this threshold (Shupe and Intrieri, 2004), as do nearly 90% of the non-precipitating liquid clouds over the tropical island of Nauru (McFarlane and Evans, 2004). The many types of clouds that may fall into this broad classification include stratus decks, cumulus fields, and mixed-phase clouds.

With such high frequencies of occurrence across the globe, these optically thin liquid water clouds are undeniably important to many different aspects of atmospheric science and are intertwined with the broader climate. Their global frequency certainly impacts the global radiative energy balance and includes the surface longwave emission in the Arctic (Shupe and Intrieri, 2004), and the shortwave albedo impact of the extensive marine stratus decks (Hartmann et al., 1992) of which many are within our definition of optically thin (cf. Zuidema and Hartmann, 1995). An intriguing feature of these clouds is that radiative fluxes are very sensitive to small changes in the LWP when the LWP is small (*e.g.*, Sengupta et al. 2003), which requires a particularly high degree of accuracy in observations and modeling. As described later, this sensitivity also presents a challenge for their accurate remote sensing. (For a further explanation, see the sidebar *Cloud Radiative Sensitivity*.)

Clouds with low liquid water paths are also intricately linked with atmospheric aerosol. The Intergovernmental Panel on Climate Change (2001) indicated that the climate forcing with the greatest range of uncertainty was that for the first aerosol indirect effect. The first indirect effect leads to an increase in the reflection of solar radiation by the cloud, whereby an increase in aerosols causes an increase in droplet concentration and a decrease in droplet size for fixed liquid-water content (Twomey, 1974). Improving our understanding of this effect in climate model simulations requires accurate observations of both the cloud LWP and  $r_e$  in association with the aerosol fields. This understanding is particularly important for the study of possible

aerosol effects on cloud lifetime, where thin clouds bookend the beginning and end of the evolution of the cloud.

### **The Challenge**

Because these clouds are optically thin, potentially mixed-phase, and are often broken (*i.e.*, have large 3-D variability), it is challenging to accurately retrieve their microphysical properties. The primary instrument for observing the cloud LWP from the surface is the microwave radiometer (MWR)<sup>1</sup>. Retrievals from the MWR are widely used because, in general: they can retrieve LWP for the wide range of values found in the atmosphere without saturating, the LWP are retrieved without requiring additional information on the cloud drop size (as do many other approaches), and it can operate 24 hours a day at a temporal resolution needed for cloud studies (*e.g.*, every 5 sec). However, recent research has found that uncertainties exist in the LWP retrievals that limit the attainable accuracy to between 20-30 g m<sup>-2</sup> (Liljegren and Lesht 1996, Westwater et al. 2001, Marchand et al. 2003, Crewell and Löhnert 2003). While a 20-30 g m<sup>-2</sup> uncertainty in the MWR-retrieved LWP is insignificant for the many clouds that have large LWPs, it represents an unacceptably large uncertainty for the thinner clouds that have a total LWP of 100 g m<sup>-2</sup> or less. The accuracy of the retrieval from the MWR is limited by: 1) uncertainties in the radiometric observations; 2) uncertainties in the gas spectroscopy (including both water vapor and oxygen) and liquid water dielectric constants used by the microwave absorption models; and 3) as for any retrieval technique, the uncertainty associated with inverting the forward model (*i.e.*, the retrieval method itself).

---

<sup>1</sup> The most common type of MWR measures the emission of microwave radiation from the atmosphere at two frequencies, 23.8 and 31.4 GHz. Using information about the atmospheric temperature profile, including estimates of the cloud temperature, the radiance measured at these two frequencies is inverted to retrieve the cloud LWP, as well as the amount of precipitable water vapor in the column.

Retrieving small LWPs ( $<100 \text{ g m}^{-2}$ ) also presents a challenge for other common remote sensing techniques that typically use the spectral information contained at visible and infrared wavelengths. Like MWR techniques, spectral infrared retrieval techniques also interpret energy emitted by the atmosphere and, in principle, can run 24 hours a day (*i.e.*, they do not need sunlight). Such infrared methods typically use spectral information from the 8-12  $\mu\text{m}$  window and can obtain simultaneous estimates of LWP and effective radius for clouds with optical depths less than about six. However, the cloud must be single-layered, the profiles of atmospheric temperature and water vapor need to be known, and the method loses sensitivity for LWPs greater than approximately  $50 \text{ g m}^{-2}$ . In the near-infrared and visible regime, methods that rely purely on the transmission of solar radiation are complicated by a pronounced nonlinear relationship between optical thickness and the reflected and transmitted fluxes, where scattering rapidly transitions from being single-scattering to primarily diffusive. This transition contains the combined influence of the cloud LWP and effective radius that must be separated. Because the dominant type of scattering changes rapidly, small measurement uncertainties can result in large uncertainties in each property. Active remote sensing by cloud radar or lidar can also provide crucial information on the vertical distribution of the cloud liquid water content (LWC; the mass of liquid water in a volume of air). However, lidars are typically limited to cloud optical depths less than about 3 or 4, above which the return signal saturates. Radars become progressively less sensitive as the cloud drop sizes and LWC decrease, and drizzle in the cloud can lead to substantial errors in the retrieved LWC.

Over the last two decades, there has been a marked increase in the number and quality of algorithms that retrieve cloud properties by taking advantage of the radiative properties of clouds in various spectral bands. Each technique may operate well under certain conditions, but thin



clouds present a particular challenge. No single technique seems able to achieve the desired accuracy and work at the high sampling rate 24 hours a day needed for cloud and climate studies. While our discussion focuses on surface remote sensing, satellite remote sensing must negotiate similar challenging issues (see top-of-atmosphere sensitivities in side bar) and, for these thin clouds, additional attention is needed for the precise depictions of the surface albedo (for visible methods) or surface skin temperature (for infrared methods). Of course, any of the methods mentioned require independent validation by techniques that can serve as a reference and, with the challenges cited, such a reference currently does not exist.

### **Addressing the Challenge: CLOWD**

One goal of the ARM Program is to use long-term observations from its CRFs to improve the parameterization of clouds and their radiative transfer in GCMs (Ackerman and Stokes 2003). Given the frequent occurrence and importance of these optically thin, liquid-water bearing clouds, ARM recently created a cross-cutting focus group called *Clouds with Low Optical (Water) Depth* (CLOWD, pronounced "klode"). One objective of this group is to compare and evaluate the different remote sensing techniques to retrieve the microphysical properties of clouds with low LWP.

We organized an intercomparison of microphysical property retrievals from a variety of methods. The immense amount of cloud data acquired at the ARM CRFs by multiple sensors provides a unique dataset that enables cross-comparisons of different remote sensing techniques. A set of 5 case study periods were selected from the ARM Southern Great Plains (SGP) site, which encompassed the range of different conditions that fall under the auspices of CLOWD (Table 1). Results from 18 different retrieval algorithms were submitted for these cases. The

participants and their retrieval algorithms are summarized in Table 2. The purposes of this exercise were to: 1) gain insight into the performance of the different algorithms, 2) identify a means to judge the accuracy of each method, and 3) isolate pressing needs required to improve these retrievals. The ultimate goal of CLOWD is to develop a robust retrieval algorithm that can be automated by the ARM program that draws on the strengths of the best methods to routinely provide accurate LWP and  $r_e$  at low LWPs for a range of possible sky conditions.

### **Results: Overcast Stratiform Case**

To simplify the discussion, the remainder of the paper will focus on one of the case study periods. A single-layer, overcast, stratiform cloud existed over the SGP CRF on 14 March 2000 (Figures 1 and 2). This case is an ideal starting point for the intercomparison, as overcast conditions reduce much of the 3-D influence on the retrieval algorithms and mitigate the possible sampling differences between the methods. Furthermore, a few of the techniques rely on diffuse radiative fields and therefore are only valid in overcast cases. This cloud is also a warm cloud, with temperatures above 5°C; so there is no ice present in the cloud to complicate the analysis. Therefore, this is perhaps the easiest case to understand in the initial CLOWD ensemble<sup>2</sup>. Although this overcast cloud lacks broken 3-D structure, it should be noted that significant internal spatial inhomogeneity exists (e.g., see Fig. 2), such that the LWP retrieved from the nine 4-km GOES pixels closest to the CRF ranges from 6 to 48 g/m<sup>2</sup> at 20:45 UTC. While this

---

<sup>2</sup> At this point, we would like to remind the reader that we are showing the results from a single case study, and therefore we should refrain from making judgements of “which algorithm is better.” To quantitatively evaluate the different methods, a large number of cases should be analyzed. However, we believe that this single example, as it was selected randomly and the results submitted by the different participants in a “blind” intercomparison activity, is representative of the uncertainty that currently exists in the techniques that are being used to retrieve LWP,  $r_e$ , and optical depth ( $\tau$ ) today.

structure deviates from that for a theoretical horizontally homogenous cloud, it is not unrepresentative for thin clouds.

#### *One MWR dataset: multiple results*

As indicated above, the main tool currently used by ARM to determine the LWP is the MWR. However, the retrieved LWP is sensitive to which absorption model is used in the retrieval (*e.g.*, Westwater et al. 2001, Marchand et al. 2003) as well as the retrieval method itself. This situation is clearly depicted in Fig 3, where four different absorption models were used along with three different techniques to retrieve LWP from the same observed MWR brightness temperatures. The resulting spread between the different LWP values is as large as  $40 \text{ g m}^{-2}$ , which represents a substantial uncertainty relative to the 0 to  $100 \text{ g m}^{-2}$  range of LWP values retrieved. This example suggests that the differences between the various algorithms are mainly biases, rather than sensitivity differences (however, different sensitivities have been noted between different absorption models [*e.g.*, Westwater et al. 2001]).

#### *One cloud radar dataset: multiple results*

The millimeter-wave cloud radar (MMCR, Moran et al. 1998) is another critical tool used to retrieve cloud properties at the ARM CRFs. The cloud radar reflectivity ( $Z$ ) observed by the MMCR is proportional to the sixth moment of the size distribution, i.e.,  $Z \sim \int r^6 n(r) dr$ . There are multiple ways to invert the radar observations and, for our relatively simple case, the four cloud radar-based methods yield significantly different results for LWP, effective radius<sup>3</sup>, and

---

<sup>3</sup> Effective radius ( $r_e$ ) is a point parameter, and profiles of  $r_e$  are retrieved by each of the cloud radar methods. However, we are comparing the mean  $r_e$  averaged over the depth of the cloud, which is more consistent with the  $r_e$  retrieved by passive methods.

optical depth (Fig 4.)<sup>4</sup>. Two of these radar methods (*aMMCR* and *mMMCR*) only use the radar reflectivity in the retrieval process, along with some assumptions, while *Microbase* and *aMMCRvod* use additional observations to help constrain the retrieval. Differences in the assumptions used in the retrieval process can result in significant differences between algorithms, as shown by the differences between the *aMMCR* and *mMMCR* results. Recall that the optical depth,  $r_e$ , and LWP are intimately related (sidebar 1) and thus a difference in the retrieved LWP between algorithms results in a difference in optical depth, provided both algorithms retrieve similar  $r_e$  values. The addition of outside information, MWR LWPs for *Microbase* and visible optical depths from the MFRSR for *aMMCRvod*, results in different solutions than the radar-only cases. Naturally, if a different MWR LWP product were used, the *Microbase* results would be affected.

### *Other techniques*

The retrievals from many of the other algorithms are given in Fig 5, which show substantial disagreement among the retrieved cloud properties. For example, Fig 5A demonstrates that differences in the retrieved LWP approach  $60 \text{ g m}^{-2}$ . However, the *MFRSR* LWP values are actually estimates of LWP derived from the *ARM Stat* MWR product. The techniques that utilize infrared observations (*MIXCRA*) and reflected visible radiation (*VISST*) retrieve significantly lower LWPs, which are in fair agreement with the *Clough Phys* MWR product, as well as with the *mMMCR* and *aMMCR* datasets.

Figure 5B shows the retrieved values of effective radius. The *lidar-radar* method, which only provides observations up to the limit of lidar signal attenuation and thus is limited to the

---

<sup>4</sup> This case avoids potential complications by large particles because the cloud is warm, and thus free of ice particles, and the low reflectivity observed by the MMCR suggests that this cloud was not drizzling and was free of insect contamination.

bottom of this cloud, has a range for the effective radii ranging from 3 to 6  $\mu\text{m}$ . The *MIXCRA v3* results, which retrieve cloud properties using radiance observations in both the 8-13  $\mu\text{m}$  and 3-5  $\mu\text{m}$  band, show similar effective radii, and the *Microbase* values are slightly larger. However, the *MIXCRA v2* (which uses only observations in the 8-13  $\mu\text{m}$  band), *MFRSR*, and *VISST* retrievals produced significantly larger effective radii.

The retrieved optical depth data are shown in Fig5C. The *VISST* and *MIXCRA v2* retrievals are in fair agreement with each other but are significantly smaller than the other algorithms. There is fair agreement between the *Microbase*, *MFRSR*, and *NFOV* retrievals, and the *MIXCRA v3* results are between.

*So which is “better?”*

Given the large spread in the results, we are left with the question “Which retrieval method yields better results for this cloud?” To this end, we constructed two “closure” experiments. In each experiment, we insert the retrieved LWP and (column averaged)  $r_e$  into a model to predict another variable, which is compared against other ARM observations. The closure experiments used include the comparison between computations using the retrieved cloud parameters and the observed broadband downwelling shortwave diffuse flux, and mean radar reflectivity at 35 GHz (panels D and E in Figs. 4 and 5). Both of these variables are sensitive to particle size and LWP; however, the radar reflectivity is more sensitive to the particle size than the LWP, while the opposite is true for the diffuse flux. Therefore, these two closure experiments complement each other and provide two bounds at which to evaluate the adequacy of the different retrievals. Note that the diffuse flux closure test is applicable since the scene is

overcast; in a broken sky scene the uncertainty associated with the cloud fraction would lead to large uncertainties in the computed fluxes.

Many conclusions can be drawn for this example in Figs 4 and 5. First, the *VISST* and *MIXCRA v2* algorithms, both of which retrieved relatively low optical depths and large particle sizes, do not close well in either diffuse flux or radar reflectivity (although for different reasons). However, the *MFRSR* method, which also retrieved a relatively large particle size, does close well in diffuse broadband flux (which was expected since it retrieves the cloud properties from the diffuse flux at 415 nm) but does not close well in radar reflectivity. This result suggests that the retrieved particle size is too large. However, if the input LWP used in the *MFRSR* algorithm were smaller (for example, if the *Clough Phys* MWR retrieval was used), then the *MFRSR*-retrieved results would have closed in both diffuse flux and radar reflectivity for this case (not shown). This case highlights the importance of having accurate LWP data to input into the *MFRSR* algorithm. The *mMMCRvod*, which also uses the diffuse flux at 415 nm as an input, also closes relatively well in shortwave flux (Fig 4D), but it does close very well with the mean radar reflectivity relative to the *aMMCR* and *mMMCR* methods.

The *MIXCRA v3* results have a similar level of agreement in diffuse flux as the *MFRSR*, and show better closure (albeit not perfect) in radar reflectivity. The inclusion of the 3-5  $\mu\text{m}$  data in the *MIXCRA v3* algorithm extends the maximum optical depth that can be retrieved to approximately 15-20, while the *MIXCRA v2* algorithm was limited to approximately 6. Both algorithms have similar sensitivity to the LWP (Fig 5A), but the inability of the *v2* algorithm to retrieve optical depths above 6 results in a positive (negative) bias in the retrieved particle size (optical depth) when the true optical depth is above this threshold.

The diffuse flux calculated using the *Microbase* retrieved properties slightly underestimates the observation and, relative to the other methods, overestimates the particle size. *Microbase* uses the radar reflectivity only in a relative sense to vertically partition the LWP from the MWR based on the normalized distribution of reflectivity with height, and the effective radius is derived from a parameterization based upon the LWC profile. This approach was chosen so to optimize the retrieval stability and accuracy over the wide range of cloud conditions found at the SGP; however, uncertainties in the MWR LWP and the parameterization are the reason why *Microbase* does not close in radar reflectivity. The primary differences between the two radar-only methods, *aMMCR* and *mMMCR*, are associated with their assumptions of the cloud drop number density. Both methods yield similar levels of closure in radar reflectivity, but do not close well in diffuse flux, with both methods yielding fluxes that are larger than the observations (implying too little LWP).

To properly judge which retrieval method yields better results, it is also necessary to obtain closure at the top of the atmosphere (TOA) because the difference between the radiation at the top and the bottom determines how much solar radiation is absorbed in the atmosphere. The broadband TOA shortwave fluxes determined from measurements by the Clouds and the Earth's Radiant Energy System (CERES, Wielicki et al. 1996) would be the counterpart to the surface diffuse flux data at the ARM site. While we do not show TOA results here, there are significant differences in TOA shortwave flux among the various retrieved products. Reconciling the discrepancies between the various retrieval techniques will require careful comparisons with a variety of closure “yardsticks” at the surface, within the atmosphere, and from space.

## Conclusions and Opportunities for Future Research

The large differences found for these state-of-the-art cloud retrievals for this simple case should serve as a rallying cry to the retrieval community to examine the accuracy of their retrieval algorithms for low LWP clouds. While thinner clouds might present complications not shared by their thicker brethren, the pervasiveness of these clouds demands that these differences be resolved for a wide variety of cloud-climate disciplines.

Where do we go from here? Because this is a single case study, more statistical intercomparisons are needed to understand the extent to which these results may be generalized. After we better understand the results for this simple case, we will examine the other case studies that have more challenging scenes, such as broken or mixed-phase clouds. These conditions will challenge not only the retrieval algorithms, but will also challenge the construction of the closure study used to evaluate the results. For example, closure in shortwave diffuse flux may not be a viable approach for evaluating the retrievals for a cumulus scene, since the uncertainty in cloud fraction might dominate the uncertainty in the shortwave cloud fluxes.

From the simple stratiform case presented here, we suggest a few prudent avenues of study. More attention is needed to resolve the significant differences that exist among the microwave absorption models, which stem from differences in the spectroscopy and cloud-water dielectric constants used, as well as the inversion approach used to retrieve LWP from the microwave radiometer. Also new methods and instrumentation are needed, which are already being developed. MWRs are being developed with different channels that enhance their sensitivity to small liquid water amounts. For example, including a 90 GHz channel reduces the MWR retrieval uncertainty from 25-30 g m<sup>-2</sup> to 15-20 g m<sup>-2</sup> (e.g., Crewell and Löhnert, 2003). However, this frequency presents its own challenges regarding instrument calibration and



uncertainties in the gas absorption model. Also, new techniques have been developed for lidar cloud property determination that use lidar returns *away* (off-beam) from where the laser beam enters the cloud (Cahalan et al., 2005; Polonsky et al., 2005). While the standard backscattering lidars are limited to clouds with optical depths less than 3 or 4, this off-beam approach does not share this limitation. As the knowledge of using active sensors matures, new research avenues arise that use them in combination. For example, Feingold et al. (2003) provide an example of how a combination of cloud radar, lidar, and other ground-based remote sensors may be used to measure the long-term effect of aerosol impact on clouds in a manner that is cost effective compared to other approaches.

We will need to pay close attention to what we consider as “truth” for the retrievals. Usually, in situ measurements from airplanes provide an agreed upon truth. However, in the case of thinner clouds, significant horizontal and vertical variability exist that complicate obtaining a representative sample. New aircraft instrumentation are being developed that would help mitigate this sampling issue by directly observing the cloud optical properties. Examples of such instruments include an airborne transmissometer (Korolev et al., 1999), a cloud extincitometer (Zmarzly and Lawson, 2000), a cloud integrating nephelometer (Gerber et al., 2000), and an in situ lidar (Evans et al., 2003, 2005). Another possibility is the expanded use of unmanned aerial vehicles (UAVs) that resemble large powered gliders and cost substantially less to operate per flight hour. Because they fly significantly slower than airplanes and can be operated longer for a given cost, cloud probes carried by UAVs would be better suited to adequately sample the cloud variability.

In the end, we need to identify a technique or set of techniques that can routinely observe the microphysical properties for all low LWP clouds. It is distinctly possible that the answer

might not lie in a single algorithm or instrument, but perhaps a conjoined algorithm must be developed. In so doing, we may need to ask: is it best to obtain a consensus solution based on a statistical combination of multiple retrieval techniques (e.g., Feingold et al. 2005), or is it best to formulate a single retrieval method that explicitly includes input from many instruments at different wavelengths? It is not clear right now which approach would be best; however, what should be clear is that a lot of interesting and vital research remains to be done.

**Acknowledgements.** This research was supported by the Office of Biological and Environmental Research of the U.S. Department of Energy as part of the Atmospheric Radiation Measurement Program.

## **Sidebar 1: Cloud Microphysics and Remote Sensing**

Drop size distribution and liquid-water content (LWC) are the two most basic properties commonly used to describe the microphysical state of a liquid-water cloud. The drop size distribution is the number of water drops as a function of drop radius. An integration of the drop size distribution multiplied by the volume of the liquid water yields its liquid-water content; i.e.,

$$LWC = \frac{4\pi}{3} \int r^3 n(r) dr.$$

Another bulk term used is liquid-water path (LWP), which is the vertical integral of the LWC through the depth of the cloud. The drop size distribution and liquid-water content can be measured in situ by airborne instrumentation. While this type of information is vital to cloud studies, aircraft flights are expensive and it is not practical to use in situ sampling to obtain the type of long-term observations needed for cloud and climate studies.

Remote sensing from the surface or satellite instrumentation can provide the needed long-term record by a variety of techniques that determine cloud properties from the radiative energy that is emitted, transmitted, or reflected by the cloud. Many remote sensing techniques cannot necessarily obtain the cloud microphysical properties directly; rather they are able to determine their radiative equivalents that are then used to infer or retrieve the cloud microphysical properties of interest. The most fundamental property that defines how a cloud interacts with shortwave and longwave radiation is its optical depth,  $\tau$ , which is an indication of the cloud opacity for a given wavelength of radiation. It is dimensionless and indicates the opacity in terms of the number of photon mean-free paths<sup>5</sup> along a vertical path through a cloud layer. For the same geometrical cloud thickness, large cloud optical depths have small mean-free paths, and vice versa. For a rule of thumb, an optical depth of ten (or greater) is approximately the point at which you can no longer see the Sun's disk through a cloud (Bohren et al. 1995). At solar and

---

<sup>5</sup> Mean-free path is the average distance a photon travels between interactions with cloud drops.

near-infrared wavelengths, where the cloud drop radii are generally much greater than the wavelength of the incident radiation, cloud optical depth can be related to LWP by (Stephens, 1994),

$$\delta \approx \frac{3LWP}{2\rho_l r_e} \quad (1)$$

where  $\rho_l$  is the density of liquid water, and  $r_e$  is the effective radius, which is the area-weighted mean radius of the cloud drops defined as,

$$r_e = \frac{\int_0^\infty r^3 n(r) dr}{\int_0^\infty r^2 n(r) dr} \quad (2)$$

where  $r$  is the drop radius and  $n(r)$  is the drop size distribution that gives the number of particles per unit volume within the radius  $r$  and  $r+dr$ . Note that the effective radius is proportional to the ratio of the volume of the cloud droplets to their projected area. Because the cloud optical depth and effective radius are obtained from remotely sensed radiative fields, they have the added advantage of being able to directly describe how clouds interact with the Earth's radiative energy balance, a key interest in climate studies.

## **Sidebar 2: Cloud Radiative Sensitivity**

Longwave and shortwave radiative fluxes are very sensitive to small changes in the cloud liquid-water path (LWP) when the LWP is small (*i.e.*,  $< 100 \text{ gm}^{-2}$ ) and thus the radiative properties of these clouds must be well understood to capture them correctly in climate models. This point is illustrated in the sidebar Figure S1, which shows radiative transfer model calculations for broadband longwave and shortwave fluxes at the surface (SFC) and top of atmosphere (TOA) as a function of cloud LWP. Solar fluxes are diurnal averages for an equinox day over a continental site a latitude of 37°N. In this example, the cloud is modeled as a uniform overcast cloud (*i.e.*, a plane-parallel, or 1-D, cloud). These plots are only intended to illustrate the climate sensitivity to cloud properties and, on a location-by-location basis, the sensitivity will vary slightly depending on additional factors including the sun angle, surface albedo, cloud height, and profile of temperature and water vapor content.

Here, the sensitivity to the atmospheric profile of temperature and water vapor content are illustrated using the standard mid-latitude summer and mid-latitude winter profiles (McClatchey et al., 1972). The warmer mid-latitude summer profile results in a greater emission of longwave fluxes at the surface and TOA, and its larger water vapor content absorbs more solar radiation and reduces the transmission of shortwave fluxes. Two effective radii are used, which are generally representative sizes for continental (6  $\mu\text{m}$ ) and maritime (12  $\mu\text{m}$ ) clouds. Fluxes are more sensitive to LWP changes for the smaller effective radii because they correspond to larger changes in optical depth. This follows from Equation 1, which indicates that optical depth is inversely proportional to effective radius, and is indicated by the dual optical depth x-axes that correspond to the same LWP axis. The longwave and shortwave sensitivities (bottom row) indicate a similar range of sensitivities for the lowest LWPs, but the longwave fluxes become

insensitive to LWP changes by  $40 \text{ gm}^{-2}$  while the shortwave fluxes continue to show some sensitivity even through  $100 \text{ gm}^{-2}$ . The sensitivities at specific wavelengths may differ, especially from those given here for the broadband fluxes, which is a feature exploited in remote sensing of cloud properties.

## References

- Ackerman, T.P., and G.E. Stokes, 2003: The Atmospheric Radiation Measurement Program. *Physics Today*, **56**, 38-45.
- Austin, R.T., and G.L. Stephens, 2001: Retrieval of stratus cloud microphysical parameters using millimeter-wave radar and visible optical depth in preparation for CloudSat. 1: Algorithm formulation. *J. Geophys. Res.*, **106**, 28233-28242.
- Barnard, J.C., and C.N. Long, 2004: A simple empirical equation to calculate cloud optical thickness using shortwave broadband measurements. *J. Appl. Meteor.*, **43**, 1057-1066.
- Bohren, C. F., J.R. Linskens, and M.E. Churma, 1995: At what optical thickness does a cloud completely obscure the sun? *J. Atmos. Sci.*, **52**, 1257-1259.
- Cahalan, R.F, M. McGill, J. Kolasinski, T. Varnai, and K. Yetzer, 2005: THOR - Cloud Thickness from Offbeam lidar Returns. *J. Atmos. Ocean. Tech.*, 22 (6), 605-627.
- Crewell S, and U. Löhnert, 2003: Accuracy of cloud liquid water path from ground-based microwave radiometry - 2. Sensor accuracy and synergy. *Radio Science*, 38 (3), Art. No. 8042.
- Donovan, D.P., and A.C.A.P. van Lammeren, 2001: Cloud effective particle size and water content profile retrievals using combined lidar and radar observations. Part 1. Theory and examples. *J. Geophys. Res.*, **106**, 27425-27448.
- Evans, K. F., R. P. Lawson, P. Zmarzly, D. O'Connor, and W. J. Wiscombe, 2003: In situ cloud sensing with multiple scattering lidar: Simulations and demonstration. *J. Atmos. Ocean Tech.*, 20, 1505-1522.

- Evans, K. F., D. O'Connor, P. Zmarzly, and R. P. Lawson, 2005: In situ cloud sensing with multiple scattering lidar: Design and validation of an airborne sensor. *J. Atmos. Ocean Tech.* (submitted).
- Feingold, G., R. Furrer, P. Pilewskie, L.A. Remer, Q. Min, and H. Jonsson, 2005: Aerosol indirect effect studies at the Southern Great Plains during the May 2003 Intensive Operations period. *J. Geophys. Res.*, in press.
- Feingold, G., W.L. Eberhard, D.E. Veron, and M. Previdi, 2003: First measurements of the Twomey indirect effect using ground-based remote sensors. *Geophys. Res. Lett.*, **30**, 1287, doi:10.1029/2002GL016633.
- Gerber, H., Y. Takano, T. J. Garrett, and P. V. Hobbs, 2000: Nephelometer measurements of the asymmetry parameter, volume extinction coefficient, and backscatter ratio in Arctic clouds. *J. Atmos. Sci.*, **57**, 3021–3034.
- Hartmann, D. L., M. E. Ockert-Bell, and M. L. Michelsen, 1992: The effect of cloud type on the earth's energy balance: global analysis. *J. Clim.*, **5**, 1281-1304.
- Intergovernmental Panel on Climate Change (2001), *Climate Change 2001: The Scientific basis - Contribution of Working Group I to the Third Assessment Report of the Intergovernmental Panel on Climate Change*, edited by J. T. Houghton et al., 881 pp., Cambridge Univ. Press, New York.
- Korolev, A. V., G. A. Isaac, J. W. Strapp, and A. N. Nevzorov, 1999: In situ measurements of effective diameter and effective droplet number concentration. *J. Geophys. Res.*, **104**, 3993–4003.



- Liljegren, J.C., and B.M. Lesht, 1996: Measurements of integrated water vapor and cloud liquid water from microwave radiometers at the DOE ARM cloud and radiation testbed in the Southern Great Plains. Internat. Geosci. Remote Sensing Symp. (IGARSS), 21-26 May, Lincoln, NB.
- Liljegren, J.C., E.E. Clothiaux, G.G. Mace, S. Kato, X. Dong, 2001: A new retrieval for cloud liquid water path using a ground-based microwave radiometer and measurements of cloud temperature. *J. Geophys. Res.*, **106**, 14485-14500.
- Lin, B., P. Minnis, A. Fan, J.A. Curry, and H. Gerber, 2001: Comparison of cloud liquid water paths derived from in situ and microwave radiometer data taken during the SHEBA/FIREACE. *Geophys. Res. Lett.*, **28**, 975-978.
- Marchand, R., T. Ackerman, E.R. Westwater, S.A. Clough, K. Cady-Pereira, and J.C. Liljegren, 2003: An assessment of microwave absorption models and retrievals of cloud liquid water using clear-sky data. *J. Geophys. Res.*, **108**, D24, 4773, doi:10.1029/2003JD003843.
- Marshak, A., Y. Knyazikhin, K.D. Evans, W.J. Wiscombe, 2004: The “RED versus NIR” plane to retrieve broken-cloud optical depth from ground-based measurements. *J. Atmos. Sci.*, **61**, 1911-1925.
- Matrosov, S.Y., T. Uttal, and D.A. Hazen, 2004: Evaluation of radar reflectivity-based estimates of water content in stratiform marine clouds. *J. Appl. Meteor.*, **43**, 405-419.
- McClatchey, R. A., and coauthors, 1972: Optical properties of the atmosphere, Environ. Res. Pap., AFCRL-72-0497, Air Force Cambridge Res. Lab., Bedford, Mass.
- McFarlane, S.A., and K.F. Evans, 2004: Clouds and shortwave fluxes at Nauru. Part I: Retrieved cloud properties. *J. Atmos. Sci.*, **61**, 733-744.

- Mie, G., 1908: Beitrage zur Optik trüber Medien speziell kolloidaler Metallösungen, *Ann. Phys.*, **25**, 377-445.
- Miller, M.A., K.L. Johnson, D.T. Troyan, E.E. Clothiaux, E.J. Mlawer, and G.G. Mace, 2003: ARM value-added cloud products: Description and status. Proceedings of the 13<sup>th</sup> ARM Science Team Meeting, Broomfield, CO. Available at [http://www.arm.gov/publications/proceedings/conf13/extended\\_abs/miller-ma.pdf](http://www.arm.gov/publications/proceedings/conf13/extended_abs/miller-ma.pdf).
- Min, Q. and L.C. Harrison, 1996: Cloud properties derived from surface MFRSR measurements and comparison with GOES results at the ARM SGP site. *Geophys. Res. Lett.*, **23**, 1641-1644.
- Minnis, P., and coauthors, 1995: Clouds and the Earth's Radiant Energy System (CERES) Algorithm Theoretical Basis Document, Volume III: Cloud Analyses and Radiance Inversions (Subsystem 4). NASA RP 1376, pp 135-176.
- Moran, K.P., B.E. Martner, M.J. Post, R.A. Kropfli, D.C. Welsh, and K.B. Widener, 1998: An unattended cloud-profiling radar for use in climate research. *Bull. Amer. Meteor. Soc.*, **79**, 443-455.
- Polonsky, I. N., S. P. Love, and A. B. Davis, 2005: Wide-Angle Imaging Lidar Deployment at the ARM Southern Great Plains Site: Intercomparison of Cloud Property Retrievals. *J. Atmos. and Ocean. Tech.*, **22**, 628-648.
- Rossow, W. B., and R. A. Schiffer, 1999: Advances in Understanding Clouds from ISCCP. *Bull. Amer. Meteor. Soc.*, **80** (11), 2261–2287.
- Sengupta, M., E.E. Clothiaux, T.P. Ackerman, S. Kato, and Q. Min, 2003: Importance of accurate liquid water path for estimation of solar radiation in warm boundary layer clouds: An observational study. *J. Climate*, **16**, 2997-3009.

- Shupe, M.D. and J.M. Intrieri, 2004: Cloud radiative forcing of the Arctic surface: The influence of cloud properties, surface albedo, and solar zenith angle. *J. Climate*, **17**, 616-628.
- Stephens, G. L., 1994: *Remote Sensing of the Lower Atmosphere*. Oxford University Press, 523 pp.
- Stephens, G.L., and coauthors, 2002: The CLOUDSAT mission and the A-Train. *Bull. Amer. Meteor. Soc.*, **83**, 1771-1790.
- Turner, D.D., 2005: Arctic mixed-phase cloud properties from AERI-lidar observations: Algorithm and results from SHEBA. *J. Appl. Meteor.*, **44**, 427-444.
- Turner, D.D., and R.E. Holz, 2005: Retrieving cloud fraction in the field-of-view of a high-spectral-resolution infrared radiometer. *Geosci. Remote Sens. Lett.*, **3**, 287-291, doi: 10.1109/LGRS.2005.850533.
- Turner, D.D., K.L. Gaustad, S.A. Clough, K. Cady-Pereira, M.J. Mlawer, J.C. Liljegren, and E.E. Clothiaux, 2004: Improved PWV and LWP retrievals from the microwave radiometer for ARM. Proceedings of the 14<sup>th</sup> ARM Science Team, Albuquerque, NM, March 22-26. Available at [http://www.arm.gov/publications/proceedings/conf14/extended\\_abs/turner3-dd.pdf](http://www.arm.gov/publications/proceedings/conf14/extended_abs/turner3-dd.pdf).
- Twomey, S., 1974: Pollution and the planetary albedo. *Atmos. Env.*, **8**, 1251-1256.
- Westwater, E.R., Y. Han, M.D. Shupe, and S. Matrosov, 2001: Analysis of integrated cloud liquid and precipitable water vapor retrievals from microwave radiometers during the Surface Heat Budget of the Arctic Ocean project. *J. Geophys. Res.*, **106**, 32019-32030.
- Wielicki, B. A., B. R. Barkstrom, E. F. Harrison, R. B. Lee III, G. L. Smith, and J. E. Cooper, 1996: Clouds and the Earth's Radiant Energy System (CERES): An Earth Observing System Experiment, *Bull. Amer. Meteor. Soc.*, **77**, 853-868.

- Zmarzly, P. M., and R. P. Lawson, 2000: An optical extincometer for cloud radiation measurements and planetary exploration. Final report submitted to NASA Goddard Space Flight Center in fulfillment of Contract NAS5-98032, 131 pp.
- Zuidema, P., and D. L. Hartmann, 1995: Satellite determination of stratus cloud microphysical properties. *J. Clim.*, **8**, 1638-1657.

## TABLES AND FIGURES

Table 1: First CLOWD Intercomparison cases<sup>†</sup>.

<b>Date</b>	<b>Time (hours UTC)</b>	<b>Comments</b>
14 Mar 2000	20:20 – 21:50	Single-layer overcast warm cloud
15 Mar 2000	17:30 – 22:30	Single-layer cumulus
11 Mar 2000	16:30 – 22:00	Single-layer cumulus (very tenuous)
12 Mar 2000	16:30 – 22:00	Single-layer, mid-level, mixed-phase cloud
13 Mar 2000	18:45 – 20:15	Mid-level water cloud below thick cirrus

<sup>†</sup> Listed in approximate order of difficulty (i.e., the first case is assumed to be easier to retrieve cloud properties and evaluate than subsequent cases).

Table 2: Algorithms and participants in the First CLOWD Intercomparison.

Type	Key Name	Contributor	Comments and [Reference]
MICROWAVE	ARM Stat	N/A	MWR LWP, standard ARM product, uses monthly retrieval coefficients determined from Liebe and Layton 1987 (dry air and water vapor) and Grant et al 1957 (liquid water) absorption model [ <i>Liljegren and Lesht 1996</i> ]
	Clough Phys	Clough, Cady-Pereira, and Turner	MWR LWP, physical-iterative method using optimal estimation, absorption model is monoRTM [ <i>Marchand et al. 2003, Turner et al. 2004</i> ]
	Lilj Stat2	Liljegren and Turner	MWR LWP, “variable coefficient” method where retrieval coefficients are predicted from surface meteorological observations; absorption model is Rosenkranz 1998 [ <i>Liljegren et al. 2001, Turner et al. 2004</i> ]
	Lin Stat3	Lin	MWR LWP, physical-iterative method using the absorption model Liebe and Layton 1987 for dry air and water vapor and Ray 1972 for liquid water. [ <i>Lin et al. 2001</i> ]
CLOUD RADAR	Microbase	Miller and Johnson	MMCR LWC and $r_e$ profiles, using the Liao and Sassen 1994 parameterization of Z-LWC and scaling the LWC profile to match the MWR’s LWP ( <i>Lilj Stat2</i> ) [ <i>Miller et al. 2003</i> ]
	AMMCR	Austin	MMCR-only retrievals of LWC and $r_e$ profiles for non-drizzling clouds, assuming a column-constant value for the droplet number density [based on <i>Austin and Stephens 2001</i> ]
	aMMCRvod	Austin	Retrieval of LWC and $r_e$ profiles for non-drizzling clouds, assuming a column-constant value for the droplet number density, from MMCR reflectivities and MFRSR-derived visible optical depths [based on <i>Austin and Stephens 2001</i> ]
	MMMCR	Matrosov	MMCR-only retrievals of LWC and $r_e$ profiles, where drizzle regions are identified by simple thresholds [ <i>Matrosov et al. 2004</i> ]
VISIBLE	MFRSR	Min	MFRSR-derived $\tau$ , and when MWR LWP ( <i>ARM Stat</i> ) is included, $r_e$ is also retrieved and more accurate retrievals of $\tau$ are realized. [ <i>Min and Harrison 1996</i> ]
	NFOV	Marshak and Chiu	Retrievals of $\tau$ from the narrow-field-of-view zenith radiometer (870 nm) [a one-channel approach similar to <i>Marshak et al. 2004</i> ]

	Not shown <sup>†</sup>	Long	Broadband shortwave retrievals of $\tau$ using an empirical relationship derived from Min and Harrison 1996. Effective radius is assumed to be 10 $\mu\text{m}$ [Barnard and Long 2004]
INFRARED	MIXCRA v2	Turner	AERI-derived $\tau$ and $r_e$ , and hence LWP, using radiance observations from 8-13 $\mu\text{m}$ [Turner 2005]
	MIXCRA v3	Turner	AERI-derived $\tau$ and $r_e$ , and hence LWP, using radiance observations from 8-13 $\mu\text{m}$ and 3-5 $\mu\text{m}$ [Turner and Holz 2005]
SATELLITE	VISST	Minnis and Khaiyer	GOES8 Visible Infrared Solar Split-window Technique applied to 10-km diameter footprint centered on the SGP site, providing $\tau$ , $r_e$ , and LWP [Minnis et al. 1995]
	Not shown <sup>†</sup>	Minnis	Terra-MODIS retrieved cloud properties [Minnis et al. 1995]
LIDAR	Lidar-Radar	McFarlane	Lidar-radar retrievals of $\tau$ and $r_e$ profiles, for cloud elements seen simultaneously by the lidar (MPL) and radar [Donovan and van Lammeren 2001]
	Not shown <sup>†</sup>	Wang	Raman lidar retrievals of $\tau$
	Not shown <sup>†</sup>	Flynn	MPL retrievals of $\tau$

<sup>†</sup> These datasets were not shown in this manuscript in order to maintain some clarity in Fig 3, 4, and 5.

## Figure Captions

Figure 1: Time-height cross-sections of radar reflectivity from the millimeter-wave cloud radar (MMCR) and elastic backscatter from the Raman lidar (RL) for the warm stratiform cloud case on 14 March 2000. A very weak low-level cloud return seen in the lidar data at 700 m between 21:15 and 21:20 UTC.

Figure 2: A sky image collected by the Whole Sky Imager on 14 March 2000 at 20:50 UTC. The sky is completely overcast; however, there is small-scale structure in the cloud field.

Figure 3: LWP retrieved from the MWR at the SGP site for the stratiform cloud on 14 March 2000 using 4 different retrieval algorithms (microwave absorption models and inversion techniques). The spread in the retrieved LWPs, all which are derived from the same brightness temperature observations, exceeds  $40 \text{ g m}^{-2}$ .

Figure 4: Retrieved LWP, effective radius, and cloud optical depth from the various algorithms that utilize cloud radar data on 14 March 2000 in panels A, B, and C, respectively. The retrieved cloud properties from each algorithm were used to compute downwelling broadband diffuse flux (D) and radar reflectivity (E), which were then compared with the observed flux and mean observed radar reflectivity (over the depth of the cloud). The “closure” exercises (gray region) provide sensitivity to primarily LWP (with shortwave diffuse flux) and particle size (with radar reflectivity). A shaded precision spectral pyranometer (PSP) provides the broadband shortwave diffuse flux observations. The spikes in the *aMMCRvod* product are caused by the presence of the very thin cloud at 700 m (Fig 1) that was filtered out of the other radar datasets.



Figure 5: Similar to Figure 4 for the retrievals that do not use MMCR data. The MWR LWP data shown in A is the *Lilj Stat2* results. Since the *Lilj Stat2* and *NFOV* methods only provide one of the three variables, and the lidar is fully attenuated by the cloud preventing LWP from being derived by the *lidar-radar* method, they were not included in the closure exercises.

Cloud Radiative Sensitivity Sidebar Figure S1. Model calculations show the sensitivity of broadband longwave and shortwave fluxes at the surface (SFC) and top of atmosphere (TOA) to cloud liquid-water path (*LWP*) and effective radius ( $r_e$ ). Optical depths corresponding to the LWP scale are given at the bottom for cloud drop effective radii of 6  $\mu\text{m}$  (solid line) and 12  $\mu\text{m}$  (dashed). The cloud is located between 900 and 1300 m in standard mid-latitude summer (red) and mid-latitude winter (blue) atmospheres. Solar fluxes are diurnal averages for an equinox day at a continental site at 37°N. The top two rows show the absolute fluxes, and the bottom row shows the flux sensitivity, in terms of the local flux difference ( $\text{Wm}^{-2}$ ) per LWP difference ( $\text{gm}^{-2}$ ). These calculations assume the sky is 100% overcast, and that the cloud does not change during the day.

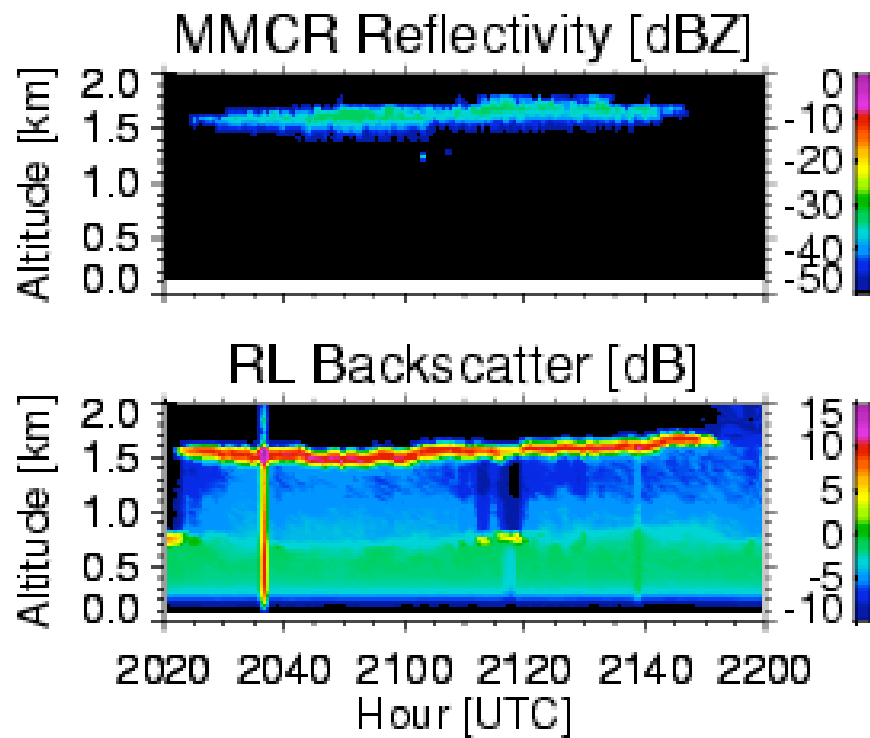


Figure 1: Time-height cross-sections of radar reflectivity from the millimeter-wave cloud radar (MMCR) and elastic backscatter from the Raman lidar (RL) for the warm stratiform cloud case on 14 March 2000. A very weak low-level cloud return seen in the lidar data at 700 m between 21:15 and 21:20 UTC.

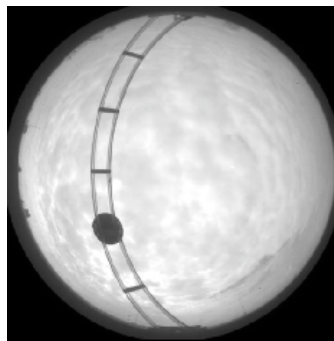


Figure 2: A sky image collected by the Whole Sky Imager on 14 March 2000 at 20:50 UTC. The sky is completely overcast; however, there is small-scale structure in the cloud field.

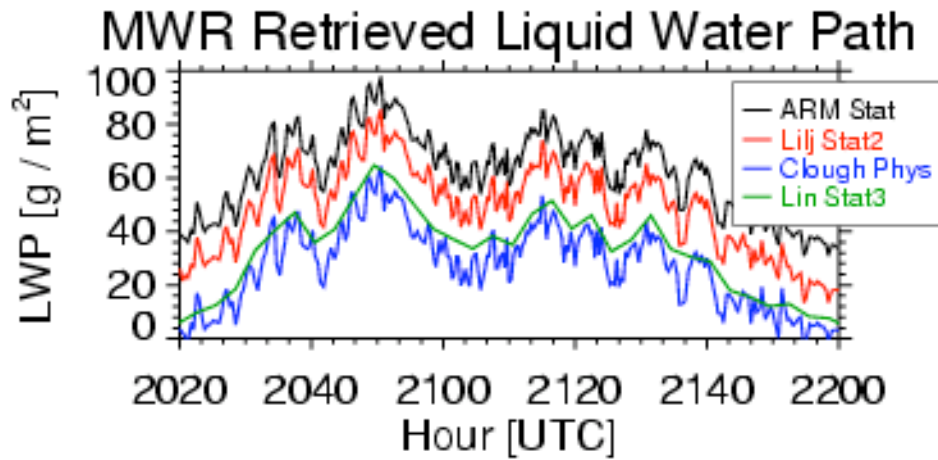


Figure 3: LWP retrieved from the MWR at the SGP site for the stratiform cloud on 14 March 2000 using 4 different retrieval algorithms (microwave absorption models and inversion techniques). The spread in the retrieved LWPs, all which are derived from the same brightness temperature observations, exceeds  $40 \text{ g m}^{-2}$ .

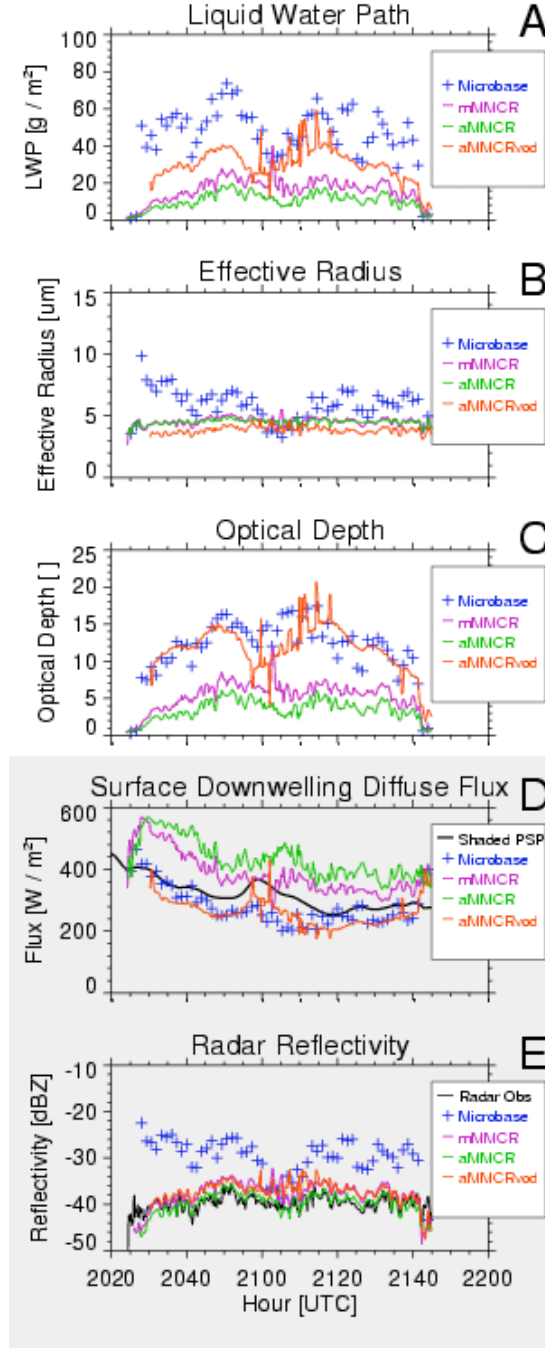


Figure 4: Retrieved LWP, effective radius, and cloud optical depth from the various algorithms that utilize cloud radar data on 14 March 2000 in panels A, B, and C, respectively. The retrieved cloud properties from each algorithm were used to compute downwelling broadband diffuse flux (D) and radar reflectivity (E), which were then compared with the observed flux and mean observed radar reflectivity (over the depth of the cloud). The “closure” exercises (gray region) provide sensitivity to primarily LWP (with shortwave diffuse flux) and particle size (with radar reflectivity). A shaded precision spectral pyranometer (PSP) provides the broadband shortwave diffuse flux observations. The spikes in the *aMIMCRvod* product are caused by the presence of the very thin cloud at 700 m (Fig 1) that was filtered out of the other radar datasets.

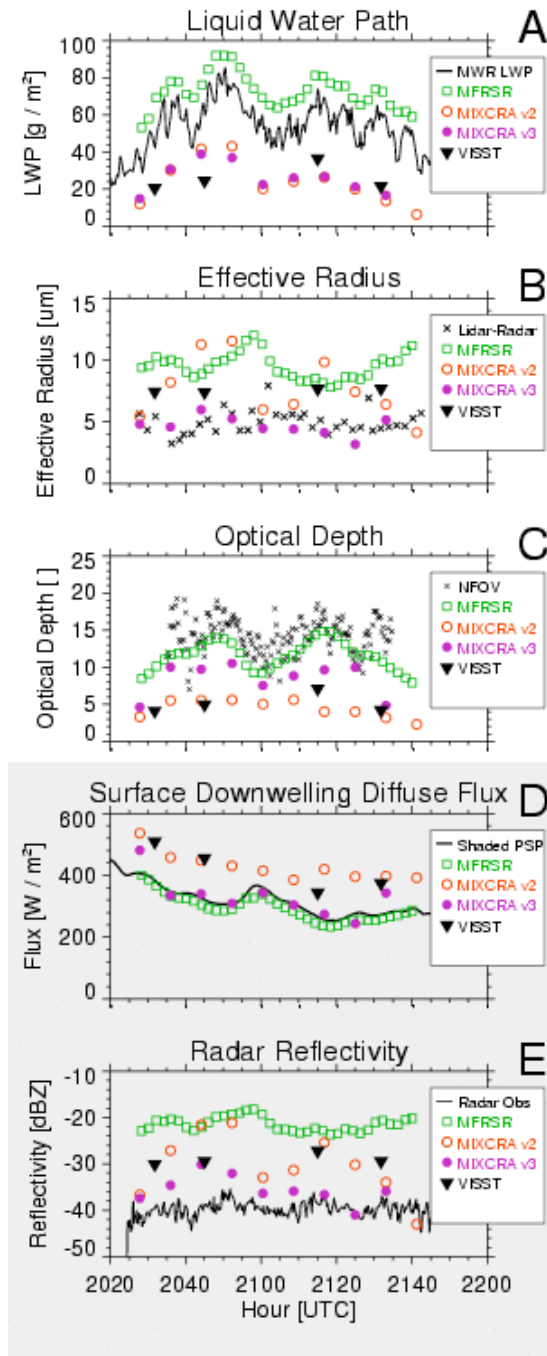
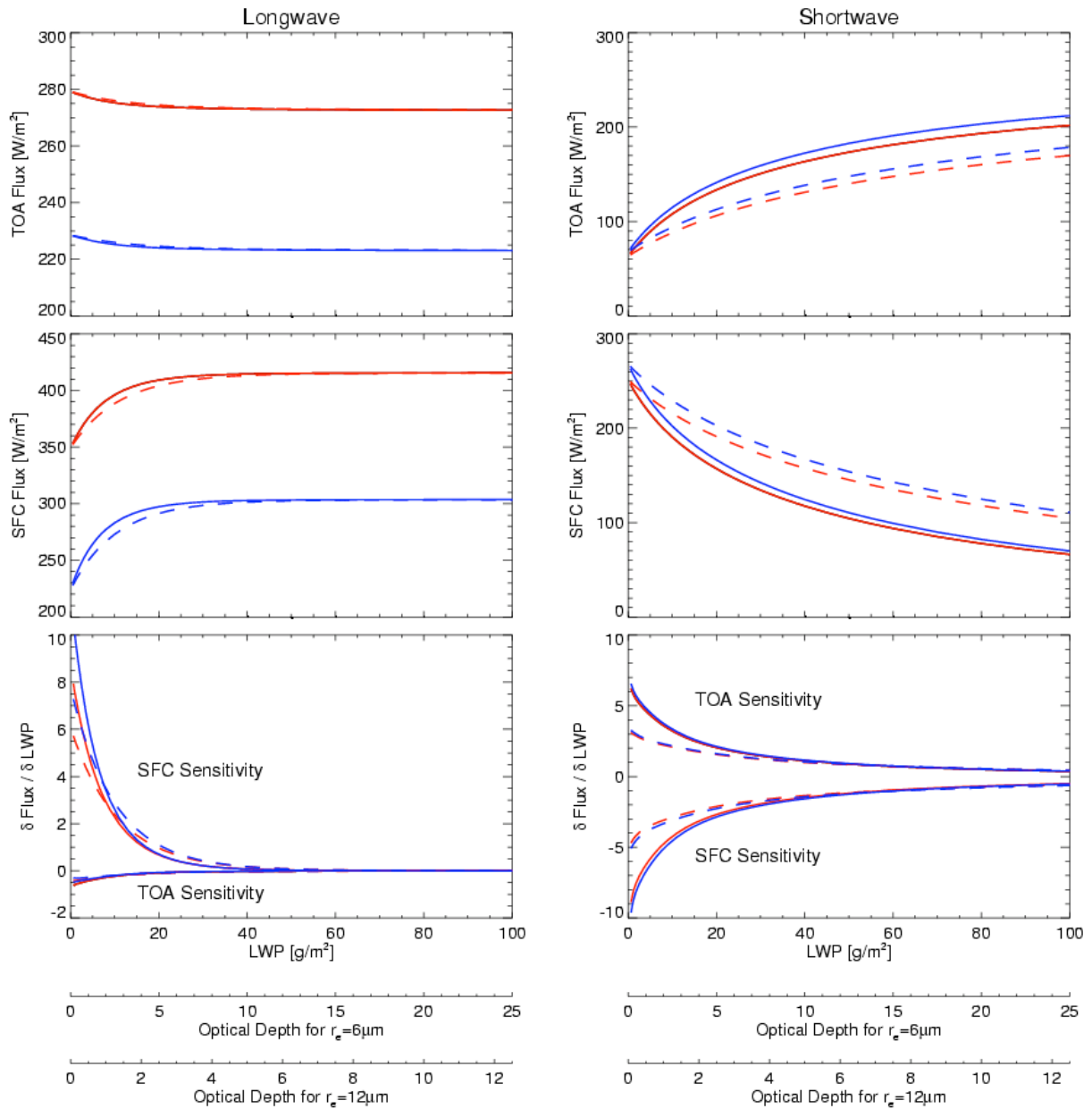


Figure 5: Similar to Figure 4 for the retrievals that do not use MMCR data. The MWR LWP data shown in A is the *Lilj Stat2* results. Since the *Lilj Stat2* and *NFOV* methods only provide one of the three variables, and the lidar is fully attenuated by the cloud preventing LWP from being derived by the *lidar-radar* method, they were not included in the closure exercises.



**Cloud Radiative Sensitivity Sidebar Figure S1.** Model calculations show the sensitivity of broadband longwave and shortwave fluxes at the surface (SFC) and top of atmosphere (TOA) to cloud liquid-water path ( $LWP$ ) and effective radius ( $r_e$ ). Optical depths corresponding to the  $LWP$  scale are given at the bottom for cloud drop effective radii of  $6\ \mu\text{m}$  (solid line) and  $12\ \mu\text{m}$  (dashed). The cloud is located between 900 and 1300 m in standard mid-latitude summer (red) and mid-latitude winter (blue) atmospheres. Solar fluxes are diurnal averages for an equinox day at a continental site at  $37^\circ\text{N}$ . The top two rows show the absolute fluxes, and the bottom row shows the flux sensitivity, in terms of the local flux difference ( $\text{Wm}^{-2}$ ) per  $LWP$  difference ( $\text{gm}^{-2}$ ). These calculations assume the sky is 100% overcast, and that the cloud does not change during the day.